

Supporting Information

Growth Mechanism of Spherical Cocrystallization of Propylthiouracil-kaempferol: New Perspectives into Surface Nucleation

*Yuntian Xiao^a, Wenchao Yang^a, Ling Zhou^{a,b,c}, Hongxun Hao^{a,b,c}, Ying Bao^{a,b,c},
Qiuxiang Yin^{a,b,c}, Chuang Xie^{a,b,c}*

^aSchool of Chemical Engineering and Technology, Tianjin University, Tianjin 300072,
PR China

^bNational Collaborative Innovation Centre of Chemical Science and Engineering
(Tianjin), Tianjin 300072, PR China

^cState Key Laboratory of Chemical Engineering, Tianjin University, Tianjin 300072, China

Contents

Table S1. Crystallographic Data and Structure Refinement Parameters for PTU-KA spherical cocrystal.

Table S2. HPLC-UV method parameters for PTU.

Table S3. HPLC-UV method parameters for KA.

Table S4. Data on the growth curve and growth rate curve in Figure 5, and liquid volume change curve in Figure 6.

Table S5. Data on the relationship between $\ln(dR_i/dt)$ and $\ln(S_i(t)-1)$ corresponding to Figure 8.

Figure S1. PXRD pattern of the PTU-KA spherulitic product compared with the patterns of PTU and KA and the calculated pattern obtained from the single crystal data.

Figure S2. Comparison of DSC plots of PTU and KA with the corresponding PTU-KA spherulitic product.

Figure S3. Comparison of TGA plots of PTU and KA with the corresponding PTU-KA spherulitic product.

Figure S4. Standard curve of PTU content (concentration-peak area) determined by HPLC-UV.

Figure S5. Standard curve of KA content (concentration-peak area) determined by HPLC-UV.

Figure S6. PXRD patterns of PTU and cocrystals after solubility experiment.

Figure S7. Spherulite morphology at complete evaporation of solution.

Figure S8. The growth of spherules at different periods in the crystallization experiment in the vial.

Figure S9. Sectional view of spherulites and high-quality single crystals masked by small crystals

Table S1. Crystallographic Data and Structure Refinement Parameters for PTU-KA spherical cocrystal.

Compound	PTU-KA
Empirical formula	C ₂₂ H ₂₀ N ₂ O ₇ S
Formula weight	456.46
Crystal system	Monoclinic
Space group	P2 ₁ /c
a/Å	15.1837(6)
b/Å	5.0298(2)
c/Å	27.6492(11)
α/°	90
β/°	105.016(4)
γ/°	90
Volume/Å ³	2039.49(14)
Z	4
ρ _{calc} g/cm ³	1.487
F(000)	952.0
Reflections collected	16080
Goodness-of-fit on <i>F</i> ²	1.023
R _{int}	0.0391
R ₁ indexes [<i>I</i> > 2σ (<i>I</i>)]	0.0347
wR ₂ indexes [all data]	0.0929
CCDC	2018929

Table S2. HPLC-UV method parameters for PTU.

Parameter	Details
-----------	---------

Column	C18 column (6 μm , 4.6 mm \times 150 mm)
Mobile phase	Acetic acid-water-acetonitrile (1: 84: 14)
Flow rate	1 ml/min
Inject volume	20 μL
Column temperature	37 $^{\circ}\text{C}$
Sample temperature	37 $^{\circ}\text{C}$
λ_{max}	275 nm
Retention time	5.2 min
Equation	$y = 113.93794x - 0.85501$
Regression coefficient (R^2)	0.9994
Calibration range	0.2 - 2.0 mg/L

Table S3. HPLC-UV method parameters for KA.

Parameter	Details
Column	C18 column (6 μm , 4.6 mm \times 150 mm)
Mobile phase	Phosphoric acid-water-methanol (2: 38: 60)
Flow rate	1 ml/min
Inject volume	20 μL
Column temperature	37 $^{\circ}\text{C}$
Sample temperature	37 $^{\circ}\text{C}$
λ_{max}	360 nm
Retention time	13.0 min
Equation	$y = 72045.45455x - 121.21978$
Regression coefficient (R^2)	0.9999
Calibration range	0.02 - 0.2 mg/L

Table S4. Data on the growth curve and growth rate curve in Figure 5 and liquid volume change curve in Figure 6.

No.	Time /s	Radius from experiment / μm	Radius from fitting / μm	Growth rate / $\mu\text{m} \cdot \text{s}^{-1}$	Solution volume from experiment / μm	Solution volume from fitting / μm
1	0	60.19	63.34	0.000298	0.50	0.5000
2	600	62.12	63.40	0.001355	0.490901485	0.4896
3	1200	64.10	63.85	0.002199	0.479188454	0.4789
4	1500	65.66	64.38	0.003257	-	0.4735

5	1800	66.87	65.19	0.004523	0.466586488	0.4682
6	2100	68.09	66.35	0.005982	-	0.4628
7	2400	69.55	67.93	0.007613	0.456546748	0.4575
8	2700	70.88	69.96	0.009386	-	0.4521
9	3000	72.16	72.51	0.011266	0.446350136	0.4468
10	3300	73.56	75.60	0.013208	-	0.4414
11	3600	75.38	79.27	0.015163	0.435212299	0.4361
12	3900	80.24	83.53	0.017080	-	0.4307
13	4200	86.49	88.37	0.018909	0.426009203	0.4254
14	4500	92.39	93.77	0.020600	-	0.4200
15	4800	103.34	99.70	0.022110	0.41555114	0.4147
16	5100	109.61	106.11	0.023405	-	0.4093
17	5400	116.72	112.94	0.024457	0.405197657	0.4040
18	5700	122.70	120.13	0.025251	-	0.3986
19	6000	131.05	127.59	0.025783	0.393432336	0.3933
20	6300	136.40	135.25	0.026057	-	0.3879
21	6600	144.42	143.04	0.026085	0.38417695	0.3826
22	6900	151.95	150.86	0.025887	-	0.3772
23	7200	158.03	158.66	0.025489	0.369535662	0.3719
24	7500	164.76	166.38	0.024918	-	0.3665
25	7800	171.16	173.94	0.024203	0.356985986	0.3560
26	8100	179.03	181.31	0.023373	-	0.3497
27	8400	184.50	188.45	0.022455	0.341821795	0.3430
28	8700	190.85	195.33	0.021475	-	0.3360
29	9000	199.11	201.92	0.020456	0.327389667	0.3287
30	9300	203.25	208.21	0.019416	-	0.3210
31	9600	211.66	214.19	0.018374	0.312434637	0.3129
32	9900	219.01	219.86	0.017342	-	0.3043
33	10200	224.35	225.21	0.016331	0.293610123	0.2954
34	10500	233.40	230.26	0.015351	-	0.2860
35	10800	237.60	235.02	0.014406	0.273896674	0.2762
36	11100	243.08	239.48	0.013502	-	0.2658
37	11400	246.77	243.66	0.012642	0.255072161	0.2550
38	11700	250.05	247.58	0.011827	-	0.2436
39	12000	252.85	251.25	0.011057	0.231018615	0.2316
40	12300	258.08	254.68	0.010333	-	0.2191
41	12600	260.76	257.89	0.009653	0.215331521	0.2059
42	12900	264.31	260.89	0.009017	-	0.1920
43	13200	266.10	263.69	0.008422	0.177734784	0.1775
44	13500	267.08	266.30	0.007867	-	0.1622
45	13800	269.60	268.75	0.007349	0.14568082	0.1462
46	14100	271.45	271.03	0.006867	-	0.1293
47	14400	272.30	273.16	0.006419	0.107508889	0.1116
48	14700	274.12	275.15	0.006002	-	0.0931

49	15000	274.89	277.01	0.005615	0.069180088	0.0736
50	15300	276.50	278.75	0.005254	-	0.0531
51	15600	277.77	280.38	0.004920	0.035661995	0.0316
52	15900	279.47	281.91	0.004609	-	-
53	16200	280.97	283.34	0.000298	-	-

Table S5. Data on the relationship between $\ln(dR_i/dt)$ and $\ln(S_i(t)-1)$ corresponding to Figure 8.

No.	$R_i / \mu\text{m}$	$S_i(t)$	$dR_i/dt / \mu\text{m}\cdot\text{s}^{-1}$	$\ln[S_i(t)-1]$	$\ln(dR_i/dt)$
1	63.34	4.03	0.000298	1.1085626	-8.118417
2	63.40	4.0696773	0.001355	1.1215724	-8.119171
3	63.85	4.1595994	0.002199	1.1504452	-6.604251
4	64.38	4.2053833	0.003257	1.1648317	-6.119667
5	65.19	4.2515077	0.004523	1.1791188	-5.726864
6	66.35	4.2977719	0.005982	1.1932471	-5.398669
7	67.93	4.3439244	0.007613	1.2071451	-5.119079
8	69.96	4.3896457	0.009386	1.2207254	-4.877947
9	72.51	4.4345289	0.011266	1.2338798	-4.668488
10	75.60	4.4780584	0.013208	1.2464742	-4.485968
11	79.27	4.5195892	0.015163	1.2583443	-4.326963
12	83.53	4.5583301	0.017080	1.2692914	-4.188911
13	88.37	4.5933336	0.018909	1.2790804	-4.069829
14	93.77	4.6234973	0.020600	1.2874397	-3.968125
15	99.70	4.6475804	0.022110	1.2940641	-3.882471
16	106.11	4.6642385	0.023405	1.2986205	-3.811715
17	112.94	4.672075	0.024457	1.3007569	-3.754826
18	120.13	4.669709	0.025251	1.3001124	-3.710846
19	127.59	4.655852	0.025783	1.2963292	-3.67887
20	135.25	4.6293863	0.026057	1.2890636	-3.658029
21	143.04	4.5894375	0.026085	1.2779955	-3.647479
22	150.86	4.5354306	0.025887	1.2628351	-3.646401
23	158.66	4.4671263	0.025489	1.2433261	-3.653997
24	166.38	4.3846321	0.024918	1.2192452	-3.669498
25	173.94	4.3500066	0.024203	1.2089623	-3.692162
26	181.31	4.2522325	0.023373	1.1793417	-3.721283
27	188.45	4.1458207	0.022455	1.1460748	-3.756189
28	195.33	4.0319413	0.021475	1.1092031	-3.796248
29	201.92	3.9118629	0.020456	1.0687931	-3.840869
30	208.21	3.7868976	0.019416	1.024929	-3.889503
31	214.19	3.6583526	0.018374	0.9777066	-3.941644
32	219.86	3.5274908	0.017342	0.927227	-3.996829
33	225.21	3.3954998	0.016331	0.8735919	-4.054632
34	230.26	3.2634715	0.015351	0.8168997	-4.114671
35	235.02	3.1323895	0.014406	0.7572432	-4.176597
36	239.48	3.0031251	0.013502	0.6947085	-4.240099

37	243.66	2.8764394	0.012642	0.629376	-4.304897
38	247.58	2.7529914	0.011827	0.5613237	-4.37074
39	251.25	2.6333511	0.011057	0.4906338	-4.437407
40	254.68	2.5180175	0.010333	0.4174052	-4.504699
41	257.89	2.4074427	0.009653	0.3417743	-4.572443
42	260.89	2.3020637	0.009017	0.2639505	-4.640485
43	263.69	2.202349	0.008422	0.1842771	-4.70869
44	266.30	2.1088682	0.007867	0.1033399	-4.776938
45	268.75	2.0224118	0.007349	0.0221644	-4.845126
46	271.03	1.944211	0.006867	-0.057406	-4.913165
47	273.16	1.8763939	0.006419	-0.13194	-4.980975
48	275.15	1.823052	0.006002	-0.194736	-5.048488
49	277.01	1.7931829	0.005615	-0.231701	-5.115647
50	278.75	1.8110042	0.005254	-0.209482	-5.1824
51	280.38	1.970779	0.004920	-0.029656	-5.248706
52	281.91	-	0.004609	-	-
53	283.34	-	0.000298	-	-

There are two points about "-" that need to be explained: (1) Since the volume of the solvent is realized by measuring the liquid level, the interval time is set to 600s; (2) When using function fitting, the value of the two points at the end is negative, so it is discarded. It is speculated that the volume of the ball at the end may interfere with the solvent volume measurement.

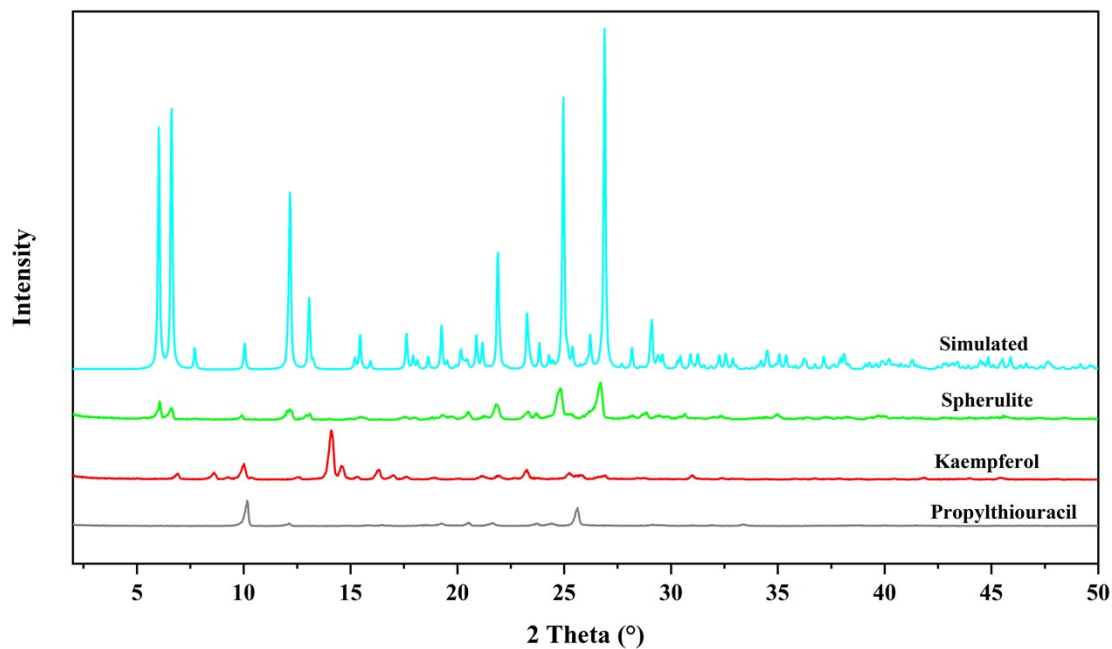


Figure S1. PXRD pattern of the PTU-KA spherulitic product compared with the patterns of PTU and KA and the calculated pattern obtained from the single crystal data.

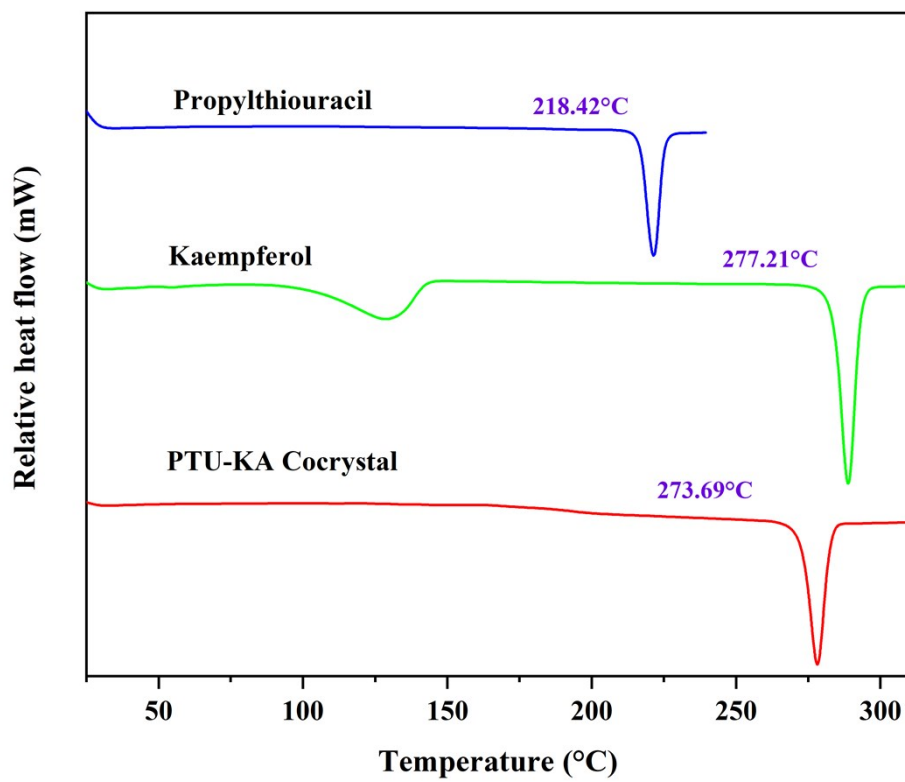


Figure S2. Comparison of DSC plots of PTU and KA with the corresponding PTU-KA spherulitic product.

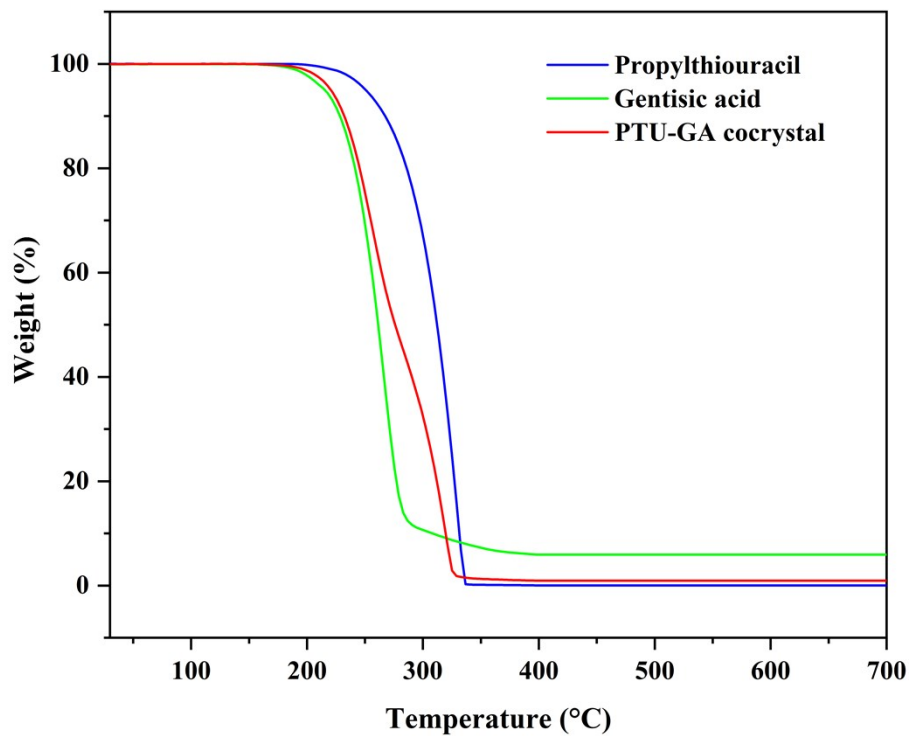


Figure S3. Comparison of TGA plots of PTU and KA with the corresponding PTU-KA spherulitic product.

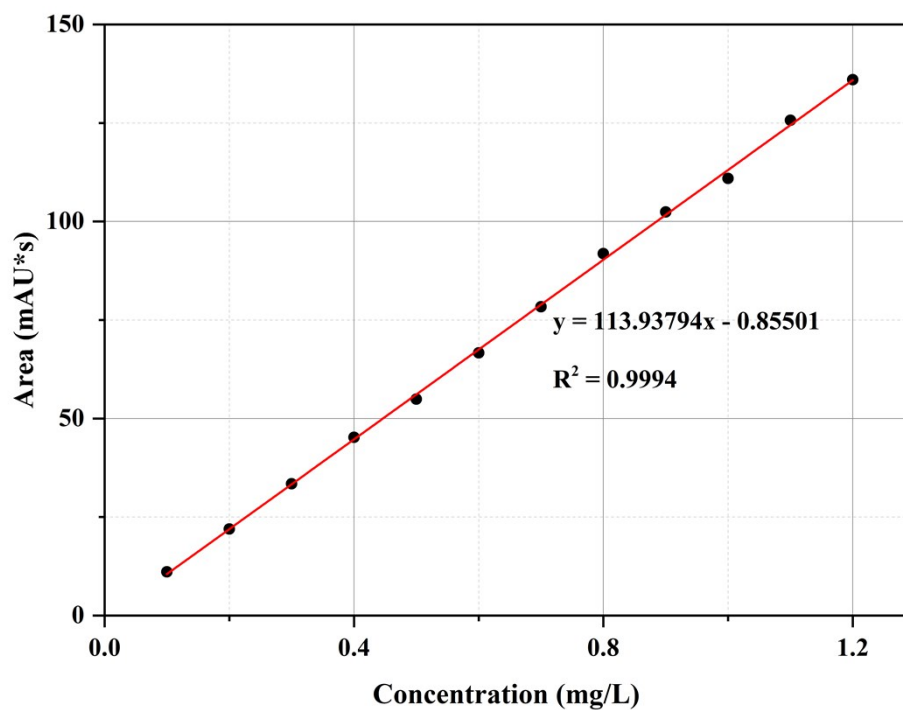


Figure S4. Standard curve of PTU content (concentration-peak area) determined by HPLC-UV.

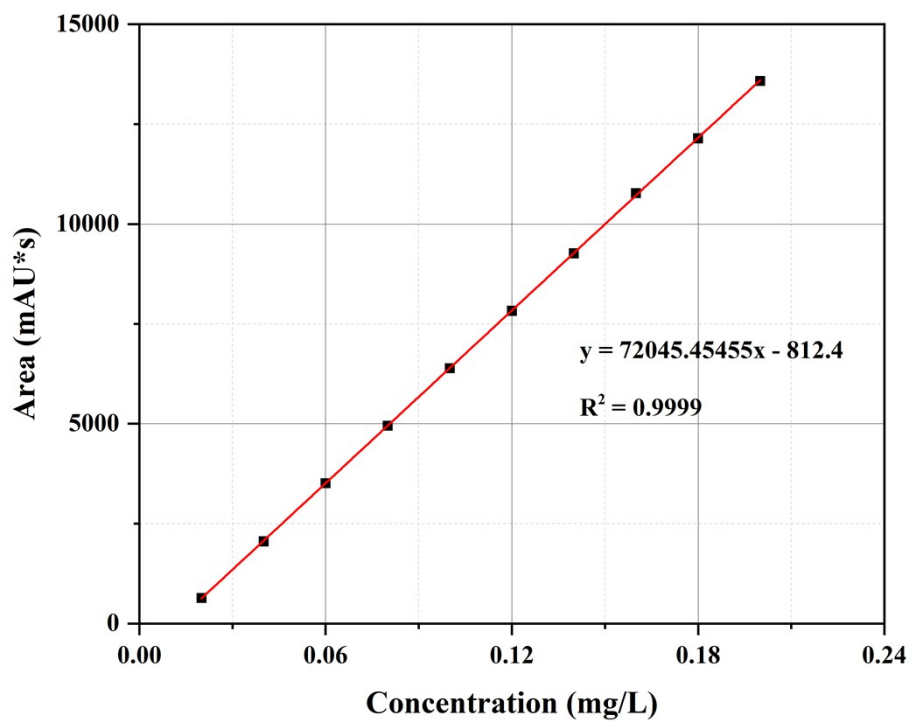


Figure S5. Standard curve of KA content (concentration-peak area) determined by HPLC-UV.

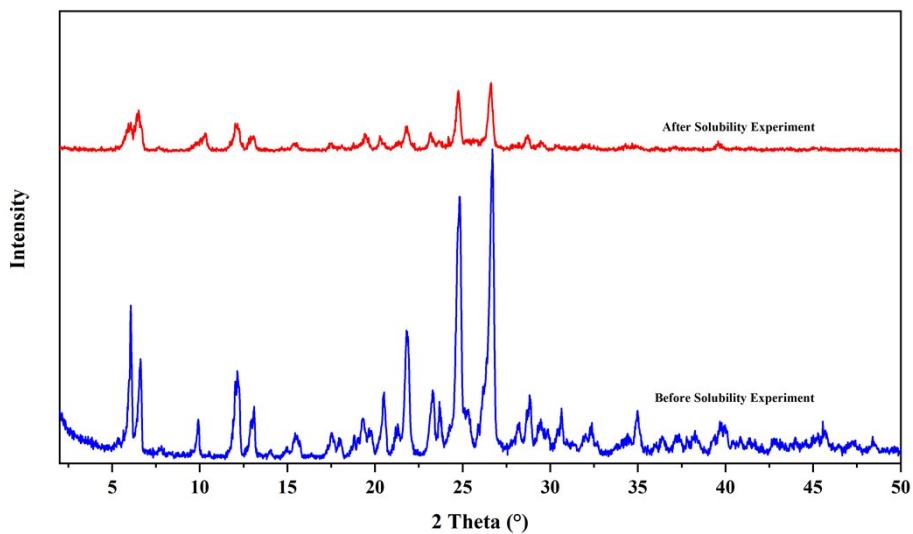


Figure S6. PXRD patterns of PTU and cocrystals after solubility experiment.

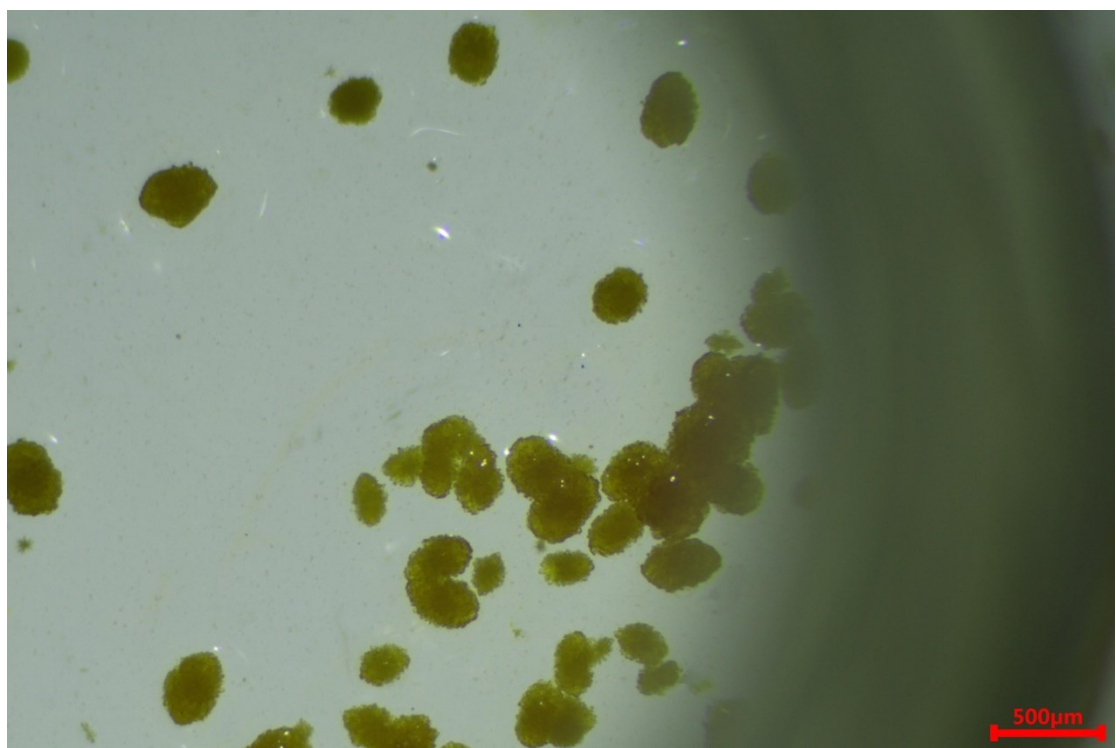


Figure S7. Spherulite morphology at complete evaporation of solution.

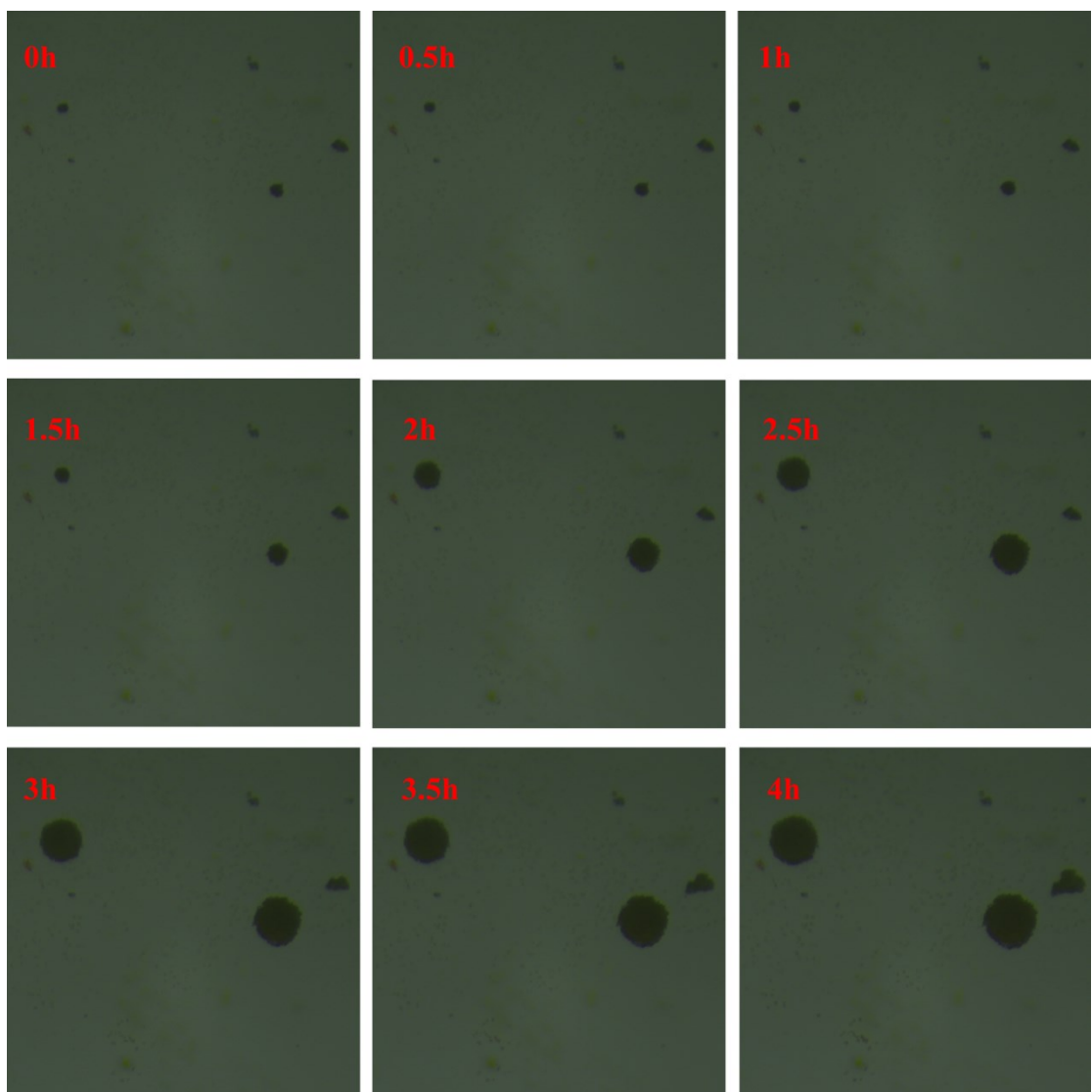


Figure S8. The growth of spherulites at different periods in the crystallization experiment in the vial.

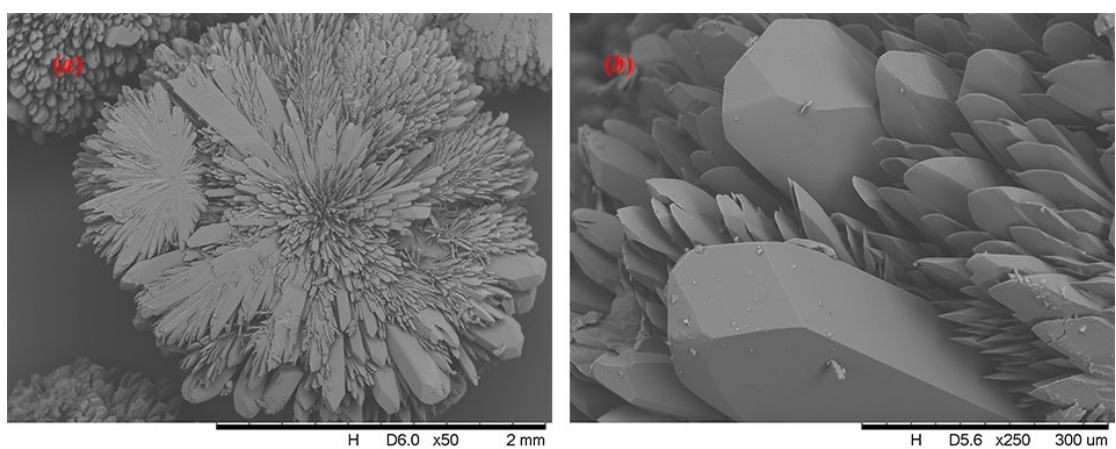


Figure S9. Sectional view of spherulites and high-quality single crystals masked by small crystals.

